Title
Initial experimental evidence of self-collimation of TNSA proton beam in a stack of conducting foils

2013-08-04

Author
Ni, PA.

Publication Date
2013-10-07

HIFAN1868

Initial experimental evidence of self-collimation of TNSA proton beam in a stack of conducting foils

by

PA. Ni, S.M. Lund, C. McGuffey, N. Alexander, B. Aurand, J.J. Barnard, F. N. Beg, C. Bellei, F. M. Bieniosek , C. Brabetz, R.H. Cohen, J. Kim, P. Neumayer, M. Roth and B.G. Logan

AFRD
Accelerator and Fusion Research Division
Ernest Orlando Lawrence Berkeley National Laboratory
Berkeley, California 94720

and
Lawrence Livermore National Laboratory, CA, USA

and

University of California, San Diego, CA, USA

and

General Atomics, San Diego, CA USA

and

GSI-Darmstadt, Germany

and
TU-Darmstadt, Germany

August 8, 2013

This work was supported by the Director, Office of Science, Office of Fusion Energy Sciences, of the U.S. Department of Energy under Contract No. DE-AC02-05CH11231.

This work was supported by the Director, Office of Science, Office of Fusion Energy Sciences, of the U.S. Department of Energy under Contract No. DE-AC02-05CH11231.

Initial experimental evidence of self-collimation of TNSA proton beam in a stack of conducting foils

[1]P.A. Ni, [2]S.M. Lund, [3]C. McGuffey, [4]N. Alexander, [5]B. Aurand, [2]J.J. Barnard, [3]F. N. Beg, [2]C. Bellei, [1]F. M. Bieniosek , [5]C. Brabetz, [2]R.H. Cohen, [3]J. Kim, [5]P. Neumayer, [6]M. Roth and [1]B.G. Logan

[1]Lawrence Berkeley National Laboratory, CA, USA
[2]Lawrence Livermore National Laboratory, CA, USA
[3]University of California, San Diego, CA, USA
[4]General Atomics, San Diego, CA USA
[5]GSI-Darmstadt, Germany
[6]TU-Darmstadt, Germany

Abstract
Phenomena consistent with self-collimation (or weak self-focusing) of laser target-normal-sheath-accelerated (TNSA) protons was experimentally observed for the first time, in a specially engineered structure ("lens") consisting of a stack of 300 thin aluminum foils separated by 50 μm vacuum gaps. The experiments were carried out in a "passive environment", i.e. no external fields applied, neutralization plasma or injection of secondary charged particles was imposed. Experiments were performed at the petawatt "PHELIX" laser user facility (E=100 J, Δt=400 fs, λ=1062 nm) at the "Helmholtzzentrum für Schwerionenforschung–GSI" in Darmstadt, Germany. The observed rms beam spot reduction depends inversely on energy, with a focusing degree decreasing monotonically from 2 at 5.4 MeV to 1.5 at 18.7 MeV. The physics inside the lens is complex, resulting in a number of different mechanisms that can potentially affect the particle dynamics within the structure. We present a plausible simple interpretation of the experiment in which the combination of magnetic self-pinch forces generated by the beam current together with the simultaneous reduction of the repulsive electrostatic forces due to the foils are the dominant mechanisms responsible for the observed focusing/collimation. This focusing technique could be applied to a wide variety of space-charge dominated proton and heavy ion beams and impact fields and applications, such as HEDP science, inertial confinement fusion in both fast ignition and heavy ion fusion approaches, compact laser-driven injectors for a LINAC or synchrotron, medical therapy, materials processing, etc.

Introduction

Focusing and collimation of space-charge-dominated ion beams ($Q \cdot R/\varepsilon^2$ >>1, where Q – perveance, R – radius, ε – emmittance) is a critical and important topic in a broad variety of applications (here and henceforth we take "ion" to refer to both ions and protons). Generally, manipulation of such beams is challenging because for a beam propagating in vacuum, the transverse defocusing electrical self-field force is much stronger than the focusing magnetic self-field force, resulting in the rapid expansion of an ion bunch (the strength ratio of electric to magnetic forces in vacuum scales as $1/\beta^2$ where β is the velocity of the beam in units of c, e.g. it is approximately 50:1 for 10 MeV protons). Common approaches to contain particles include application of strong external fields (magnetic or electric), propagation of ions through low-density plasma, etc. [1,2,3,4,5,6].

Presently, a number of different approaches have been evaluated specifically for focusing and collimation of high current density, laser-driven TNSA proton beams. These methods include different techniques such as ballistic focusing with a curved source foil, electrostatic focusing resulting from charging of a metal structure by co-moving or laser-generated electrons, externally applied fields from permanent magnet quadrupoles or pulsed solenoids, etc. [1,7,8,9,10,11].

The stack focusing technique we describe here could be a better alternative in the future, however *the main point of the present work is the first-time observation of the self-focusing in laser-driven heavy ion beams consistent with passive magnetic focusing*. In general we see the method applicable to other species of ions, such as carbon, deuterium, iron, etc., accelerated either by the TNSA, the Break-Out Afterburner (BOA), or similar mechanisms. Potential applications include HEDLP science, inertial confinement fusion fast ignition, inertial confinement heavy ion fusion, a compact laser-driven injector of a LINAC or synchrotron, cancer therapy, materials processing, neutron and positrons generation etc.[12,13,14,15,16,17,18,19,20,21,22].

Recent theoretical work[23,24], showed that the self-focusing phenomenon could occur in a TNSA proton beam when it propagates through a structure consisting of stacked thin conducting foils separated by insulating gaps. Briefly, as a TNSA proton beam propagates ballistically from the source foil, it is charge-neutralized by co-moving hot electrons; the net current is zero. In the proposed scheme, all the co-moving electrons are stopped within the first few foils of the stack, and as a consequence the resulting proton beam is strongly space-charge-dominated with a large positive net current. This is an unusual situation, since in most cases effort is made to avoid an unneutralized beam with such high space-charge intensities. As the beam propagates through the stack, an image charge builds at each foil, generating an electric field that counteracts (or "neutralizes") the electric field of the beam (or in other words the conducting boundary conditions at the conducting foils result in a reduction in the transverse electric field). Meanwhile, because of the residual finite resistivity, the foils do not affect the self-magnetic field of the intense beam, thus making net focusing possible. It was found that the degree of the electrical field neutralization depends on the aspect ratio between beam transverse size (e.g. radius) and that of the gap between foils (see Figure 1 in[24]). For a typical TNSA proton beam, references [23] and [24] show that the idealized degree of focusing can range from partial collimation to a very strong pinch. Due to proton inertia and the typical magnetic self-field strength, proton trajectories can be bent noticeably in a distance of several tens of millimeters. As a consequence, the number of foils necessary to maintain the E-field neutralization at such large spatial scales ranges from ~100 to ~1000.

In the experimental work described here, we designed and fabricated a robust target aimed at observing the anticipated phenomenon guided by the theoretical work[24]. Since complexity of a lens (i.e. number of foils, size of the gap, etc.) strongly depends on focal length/strength, a stack was configured for a moderate focusing, in which the beam makes an overall expansion but the expansion rate is decelerated to a measurable degree, – an intermediate "tuning" that requires a smaller number of foils and reasonably large gaps thus resulting in less manufacturing effort and lower cost of a target. (From here on, under the term "focusing" it is understood when the beam is focused relative to what it would have been without the lens). Multiple physics phenomena, such as beam stopping, beam straggling, knock-on electrons dynamics, foil heating mechanical strength, and short pulse beam effects had to be considered in the design.

In this work we exploit a passive focusing approach, in which only the self-fields of the beam are used: the defocusing self-electrical field of the beam is attenuated by the foil structure, while the focusing magnetic field is unaffected allowing net focusing of the beam. Similar magnetic self-focusing phenomenon or "pinch focusing" is well known in MeV-energy electron beams: at these energies, the $1/\beta^2$ factor for relativistic electrons readily approaches unity rendering magnetic focusing easier than for ions. To date, few experimental demonstrations of self-focusing in ion beams have been documented[25]. The primary impediment is the lack of heavy ion beams with sufficiently high current and relatively low emmitance. In this respect, a TNSA-produced proton beam[26] provides a good opportunity to experimentally study the phenomena with existing laboratory facilities: proton currents are high (10s of kilo-Amperes) and emittances are low ($\leq 0.1\pi$ mm·mrad)[27].

Experimental setup

The target and experiment design are extensively covered in[24] and is illustrated in Figure 1. Experiments were performed at the PHELIX laser user-facility at "Helmholtzzentrum für Schwerionenforschung–GSI", Darmstadt, Germany. A proton beam was generated by a 100 J, 400 fs FWHM, 1062 nm PHELIX laser pulse. The resulting ion bunch had a typical exponential-like energy spectrum extending to 20

MeV in axial kinetic energy. The initial pulse duration of the beam was approximately 5ps, corresponding to ~0.5 MA average proton current over the pulse. A focusing target consisted of a stack of 300, circular (12 mm diameter), 650 nm-thick, aluminum foils, separated by 50 μm-vacuum gaps (target chamber pressure P=10^{-6} mbar). The target housing as well as all of the foils were electrically grounded at the radial periphery of the structure. 100 μm diameter holes were drilled at the outer radial edge of each foil to allow the gaps between the foils to pump down in the target chamber and prevent their damage during chamber evacuation.

A TNSA proton beam accelerated from a flat foil typically has large angular divergence -- up to 40˚ in full angular extent. As it was discovered in the earlier work[23], a key requirement for the lens to show a clear signature of passive focusing is a collimated or slightly converging proton beam envelope at the lens entrance. This requirement stems from the magnetic focusing term becoming stronger under tighter radial focusing so an initially radially diverging beam will require much more propagation distance (i.e. more foils) for the weaker magnetic term to overcome the envelope divergence to produce a clearer signature of magnetic focusing. We attempted to produce this injection condition by employing a curved "source" foil (gold partial sphere 300 μm radius of curvature, 10 μm thick, mounted on an insulating glass stock) used instead of a flat foil[7,12]. The laser was focused to a 75 μm-diameter focal spot where the centerline normal to the first foil of the target intercepts the hemisphere foil spaced 400 μm downstream (see Figure 1). LSP simulations and theory[28] suggest that this foil curvature and spacing result in a quasi-collimated proton beam envelope in the 10 MeV-20 MeV portion of the beam impinging on the first foil of the focusing lens. Unfortunately, considerable uncertainty resulting from uncertain initial distribution parameters together with substantial 20% shot-to-shot jitter in the laser pulse likely renders this collimation tuning very approximate. Nevertheless, it appears to have substantially reduced the characteristic 40˚ angular spread seen in previous TNSA experiments[7].

The overall goal of the experiment is to measure a clear passive magnetic focusing effect from the foil stack on the proton beam. For this purpose two types of experiments were performed: first, a "reference" shot (Figure 1a), in which the space charge-dominated beam was expanding freely in vacuum after passing through one thick foil, and second the focusing "lens" shot (Figure 1b) using the previously described lens consisting of a stack of 300 thin foils. A target for the reference experiment was identical to the lens one, but the 300 thin foils were replaced by a single, 195-μm-thick foil which is equal in thickness to all the foils in the stack and the left edge of the thick foil is placed at the axial location where the foil stack begins. The equivalent thickness results in approximately the same accumulated beam distortions, such as the energy losses, straggling, and scattering, and most importantly the same space-charge conditions, since the single thick foil absorbs all the neutralizing electrons, as will the first few foils in the foil stack lens. Comparison of reference and stacked foil lens shots should determine the effect of the stacked foil structure on an otherwise identical beam. These assumptions are supported by theoretical analysis presented in[23,24].

A stack of radio-chromic films (RCF), intermixed with 100 μm-thick aluminum filters served as the main diagnostic for the transverse beam size measurement[7,29] . Because higher energy protons deposit deeper within the RCF stack and the TNSA produced proton beam has a broad, exponential-like energy spectrum, exposures measured in the RCF stack allow reconstruction of the rms radial extent of the beam as a function of proton energy for each shot (higher energy data is most reliable in the analysis to reconstruct the beam size).

The effect of the lens on the beam divergence was determined by comparing an rms measure of the radial beam diameter in the reference shot to that in the lens shot (see example shots in Figure 1c). Based on simple geometric optics considerations, the relative difference in spot size is largest when the RCF films are placed at the axial position where the beam exits the foil lens. However the flux density at this position is still too high, resulting in burning and overexposure of films. It was found that a ~7 mm axial gap downstream of the foil lens is the shortest distance at which it is still possible to make measurements without overexposing films. Upon exiting the lens, the unneutralized proton beam drifts in vacuum and should experience a rapid radial expansion, caused by the space-charge forces.

Experimental results

The radius of a circle containing 90% of the particles (dose) in the two experiments is plotted versus "RCF energy" in Figure 2. The "RCF energy" approximates the initial energy of a proton that decelerated in the aluminum and stopped completely in a sensitive layer of a corresponding RCF film. To extract dose information with the highest possible dynamic range, the beam profiles were analyzed using the green channel of RGB scanned films[29].

The reduction of spot size in the experiment with a stack is apparent in data plotted in Figures 1c and 2: the foil lens significantly diminished the expansion of the proton beam relative to the reference target. The effect is stronger for lower proton kinetic energies with the effective focusing factor ranging from a value of 2 at 5.4 MeV to a value of 1.5 at 18.7 MeV. We note that a TNSA proton beam inherently has the inverse dependence of radial spot size on energy; hence the comparison to the reference shot is the correct way to separate the effect of the lens from the "pre-exiting" structure of the distribution as a function of energy. In overall, in our experiment, the proton beam size is smaller at the extended distance (22 mm), which would not possible without the lens.

A detailed simulation is necessary to probe the internal dynamics of the beam inside the lens that is beyond the scope of this paper. For now, the stronger focusing at lower kinetic energies can be plausibly explained by the exponential energy spectrum: the beam current is higher at lower energies, leading to a stronger self-magnetic focusing force due to the contribution to the magnetic field by more numerous protons at lower energy. In addition, the initial distribution of protons impinging on the foils at the lower energies has a larger initial radius[28] leading to an aspect ratio corresponding to a higher degree of electrical field attenuation[23]. Finally, at lower energy there is more time for electrostatic repulsion to act upon the beam before depositing in the diagnostic film; even at the same current, one would expect more expansion at lower energy in the reference case, and hence reduction of the self-electric field in the foils should have a larger effect.

The dose deposited by the beam in each film of the RCF stack can be calculated from the known exposure characteristics of the film[29]. Data obtained for a reference shot and foil lens shot are shown in Figure 3 with estimated error bars. Note that error ranges are less for higher kinetic energies due to the those groups primarily depositing in deeper films with less exposure which results in less error in backing out the measure from calibrated exposure characteristics. Within the error-bar range, the total deposited energies of the reference and foil shots can be considered the same. Although this is an expected outcome, it supports assumptions made earlier for the reference targets having proper equivalency to allow relative comparisons to foil targets to derive an effective focusing strength.

Data on the reproducibility of focusing characteristics in multiple shots (both lens and reference) is summarized in Figure 4. The effective angular divergence plotted corresponds to the angle between the line from center of the source to the center of the RCF stack and the line from the center of the source to the average radius of a beam. Although, this measure does not reflect the true local divergence of the beam envelope, it further contrasts the difference between lens- and reference-shots. Note that despite there is considerable shot-to-shot variation likely associated with the variability in the laser pulse (20% jitter) and precision of target dimensions (5%), the overall statistics support the conclusion that the stack does affect the beam envelope of the proton beam in the predicted “focusing” fashion.

Discussion

The principle difference between the present foil focusing experiment and earlier experiments on beam focusing with magnetic pinching[25] is in the way the self-electric field is neutralized. In Ottinger et al.’s work a proton beam was propagated through a low-density neutral gas (P=10^{-2} mbar); slow-moving electrons, generated during collisional ionization of the gas, effectively neutralized the space charge of the beam but not the focusing magnetic field. In contrast, in the foil lens concept, the image charges on conductors are responsible for the self-electric field neutralization as explained in[23]. The primary advantage of the foils is that the self-electric field neutralization can be better controlled with the foils without significant damage to the ion distribution and the foils suppress electrons from co-moving with the ion beam that can complicate various applications.

The physics in the experiment is complex as it contains elements of beam physics, beam matter interaction, low-density plasma, warm-dense-matter, etc. There is no diagnostic that could measure the beam dynamics inside the lens directly was at our disposal. Extensive numerical modeling of experiments with a code that includes the relevant physics issues and matches the experimental data collected at the end of the lens could provide the necessary insight and guide future experiments. In previously reported numerical modeling efforts of foil focusing using the Warp code[23], only beam physics aspects were considered; issues associated with the initial distribution were idealized and both knock-on electrons and scattering induced by the foils were not addressed. There is an ongoing integral simulation effort that includes most of the effects, results of which will be reported in future publications. In the present study, we provide qualitative arguments that support the assumption that reduction of the repulsive electrostatic forces together with magnetic self-focusing are the dominant mechanisms responsible for the observed data.

There are several potentially confounding phenomena different from the magnetic self-focusing that could affect the beam dynamics [24]. Firstly, a low-density plasma channel could form on the path of the proton beam. There are three potential sources of plasma: knock-on electrons; hot expanded, under-dense, evaporated foil material; gas desorbed from the foils and impact-ionized by the beam. Propagation through such plasma could result in current and space-charge beam neutralization, self-focusing, filamentation, instabilities, electrical shortening of foils etc. Secondly, the foils could charge up (by earlier energetic electrons in the expanding TNSA-produced plasma, absorbed and emitted knock on electrons, etc.), resulting in strong electrostatic fields that can affect particle dynamics. In following we present estimates that these effects are unlikely to affect the beam, making the magnetic focusing the primarily physics mechanism.

Knock-on electrons are generated during impact of protons with a metallic foil. Electrons liberated can accumulate and form an electron plasma cloud, co-propagating with the beam and neutralizing it. Our estimations predict that contribution of knock-on electrons is negligible for protons with kinetic energies roughly 8 MeV and above. The average number of electrons, generated per one collision of a 10 MeV proton with a 650 nm-thick aluminum foil, is ~0.01 [30]. However, in spite of this small number, electrons could build up over multiple foil interactions. Our estimated energy of knock-on electrons is in the keV-range based on the assumption that few percent of the energy from an MeV-energy proton is transferred to an electron. Meanwhile, per electron cold stooping values, a single 650 nm thick foil is sufficient to absorb most electrons in this range and as a consequence, the generated electrons cannot propagate beyond a few foils and build up.

A low-density plasma is likely to appear in the foil structure, but it may become significant only after the high energy portion of the beam of interest has already passed through the stack. Slightly ionized, low-density aluminum plasma is created as foils get heated by the beam and expand hydrodynamically. The relatively tenuous, high-energy portion of the beam in the earlier part of the pulse does not deposit enough energy in the foils to melt Aluminum. More numerous protons below 5 MeV impinge on the foils later and do most of the heating. Estimates show that their energy is sufficient to evaporate the foils by heating them to 1-2 eV peak temperature. Cold stopping is the dominant mechanism, because much higher temperatures (>100 eV) are required to produce a significant increase in dE/dx stopping[31]. The characteristic time for hydro-motion for a 650 nm thick foil is ~1000 ps, while it takes approximately 300 ps for the entire bunch (including the low energy portion) to travel through the entire 15-mm-long foil stack. Thus, due to the very short proton pulse and broad energy spectrum, the peak temperature is only reached by the time the most of the beam has passed though the stack.

Electrostatic focusing/defocusing effects can appear as the result of foils charging by the balance of absorbed and emitted electrons, photo ionization, etc. Ideally, the common grounding of all foils should prevent undesired net charging of individual foils. However, on very short time scales, free electrons in the foil metal may not have sufficient time to respond, thus creating transient electric fields. A precise description of this phenomenon is difficult but it is possible that this effect is not large in our experiments, since the beam duration (~5 ps) is still much longer than the ~0.001 ps inverse plasma frequency of electrons in a metal, – the shortest reaction time of electrons to an external potential.

Lastly, high-energy MeV electrons are also created during the laser plasma interaction in the TNSA process. These electrons have several millimeters ranges and thus pass through the stack. However, the speed of these electrons is much higher than that of protons and their effect can be neglected.

Summary

A significant reduction in divergence of a TNSA-produced proton beam was experimentally observed for the first time using a passive stacked-foil lens. The observed spot size reduction depends on energy, with the effective focusing factor decreasing monotonically from a value of 2 at 5.4 MeV to a value of 1.5 at 18.7 MeV. The experimental evidence presented here supports the simple interpretation posed in previous plausibility[24] and theoretical studies[23] with the foils simply attenuating self-electric defocusing forces in the beam to allow passive magnetic focusing. Results suggest a lack of confounding effects from undesired plasma neutralization etc. This lays the groundwork for follow-on investigations of the technique both experimentally and in modeling/simulations to more complete viability testing of this new ion focusing technology. The substantial promise of the foils to block co-moving electrons associated with TNSA produced proton beams and the favorable scaling of the focusing strength derived from self-magnetic fields of the beam (pinch-type focusing) is highly desirable for a broad range of applications and motivates next-step verification.

Acknowledgments

The authors would like to thank Joe Kwan (LBNL), Alex Friedman (LLNL), Harry McLean (LLNL), Prav Patel (LLNL) and Gabriel Schaumann (TU-Darmstadt) for fruitful technical discussions. We also want to thank the technical team of PHELIX for support of the experiments and General Atomics for providing the targets for the experiments. The authors sadly note the untimely passing of our friend, colleague, and co-author Frank Bieniosek. His clarity of scientific vision, his energy and enthusiasm, guidance, and companionship are missed. This research was performed under the auspices of the U.S. Department of Energy at the Lawrence Berkeley and Lawrence Livermore and National Laboratories under contract numbers DE-AC02-05CH11231 and DE-AC52-07NA27344 and was partially supported by the US DOE, OFES, under HEDLP proposal #DE-FOA-0000583.

References

[1]K. Harres, I. Alber, A. Tauschwitz, V. Bagnoud, H. Daido, M. Günther, F. Nürnberg, A. Otten, M. Schollmeier, J. Schütrumpf, M. Tampo, and M. Roth, *Phys. Plasmas* **17**, 023107 (2010)

[2]Nishiuchi, H. Sakaki, T. Hori, P. R. Bolton, K. Ogura, A. Sagisaka, A. Yogo, M. Mori, S. Orimo, A. S. Pirozhkov, I. Daito, H. Kiriyama, H. Okada, S. Kanazawa, S. Kondo, T. Shimomura, M. Tanoue, Y. Nakai, H. Sasao, D. Wakai, H. Daido, K. Kondo, H. Souda, H. Tongu, A. Noda, Y. Iseki, T. Nagafuchi, K. Maeda, K. Hanawa, T. Yoshiyuki, and T. Shirai *Phys. Rev. Accel. Beams*, **13**, 071304 (2010).

[3]M. Basko, A. A. Drozdovskii, A.A. Golubev, K. L. Gubskii, D. D. Iosseliani,. A. V. Kantsyrev, M. A. Karpov, A. P. Kuznetsov, Yu. B. Novozhilov, O. V. Pronin,. S. M. Savin, P. V. Sasorov, D. A. Sobur, B. Yu. Sharkov, and V. V. Yanenko, *Phys. Part. Nucl. Lett.* **5**, 582–585 (2008).

[4]A. Tauschwitz, E. Boggasch, D.H.H. Hoffmann, J. Jacoby, U. Neuner, M. Stetter, S. Stöwe, R. Tkotz, M. De Magistris and W. Seelig, *Laser Part. Beams* **13**, 221–229, (1995).

[5] P.A. Seidl, A. Anders, F.M. Bieniosek, J.J. Barnard, J. Calanog, A.X. Chen, R.H. Cohen, J.E. Coleman, M. Dorf, E.P. Gilson, D.P. Grote, J.Y. Jung, M. Leitner, S.M. Lidia, B.G. Logan, P. Ni, P.K. Roy, K. Van den Bogert, W.L. Waldron, D.R. Welch, *Nuclear Instruments and Methods in Physics Research Section A: Accelerators, Spectrometers, Detectors and Associated Equipment*, **606**, Issues 1–2, Pages 75–82 (2009)

[6]S. Ter-Avetisyan, M. Schnürer, R. Polster, P. V. Nickles, and W. Sandner, *Laser Part. Beams*, **26**, 637–642, (2008).

[7] Teresa Bartal, Mark E. Foord, Claudio Bellei, Michael H. Key, Kirk A. Flippo, Sandrine A. Gaillard, Dustin T. Offermann, Pravesh K. Patel, Leonard C. Jarrott, Drew P. Higginson, Markus Roth, Anke Otten, Dominik Kraus, Richard B. Stephens, Harry S. McLean, Emilio M. Giraldez, Mingsheng S. Wei, Donald C. Gautier & Farhat N. Beg *Nature. Phys*., **8** 139 (2011), and references therein.

[8]M. Schollmeier, S. Becker, M. Geißel, K. A. Flippo, A. Blažević, S. A. Gaillard, D. C. Gautier, F. Grüner, K. Harres, M. Kimmel, F. Nürnberg, P. Rambo, U. Schramm, J. Schreiber, J. Schütrumpf, J. Schwarz, N. A. Tahir, B. Atherton, D. Habs, B. M. Hegelich,

and M. Roth, *Phys. Rev. Lett*. **101**, 055004 (2008).

[9]H. Ruhl, T. Cowan, J. Dahlburg, P. Parks and R. Stephens, *Nucl. Fusion* **44**, 438–442 (2004).

[10] O. WILLI, T. TONCIAN, M. BORGHESI, J. FUCHS, E. D'HUMIÈRES, P. ANTICI, P. AUDEBERT, E. BRAMBRINK, C. CECCHETTI, A. PIPAHL and L. ROMAGNANI, *Laser and Particle Beams* **25**, 71–77 (2007).

[11] S. N. Chen, E. d'Humières , E. Lefebvre, L. Romagnani, T. Toncian, P. Antici, P. Audebert, E. Brambrink, C. A. Cecchetti, T. Kudyakov, A. Pipahl, Y. Sentoku, M. Borghesi, O. Willi, and J. Fuchs, *Phys. Rev. Lett.* **108**, 055001 (2012).

[12]P. K. Patel, A. J. Mackinnon, M. H. Key, T. E. Cowan, M. E. Foord, M. Allen, D. F. Price, H. Ruhl, P. T. Springer, and R. Stephens, *Phys. Rev. Lett*. **91**, 125004 (2003), and references therein.

[13]Henestroza, B. G. Logan, and L. J. Perkins, *Phys. Plasmas* **18**, 032702 (2011).

[14]M. Roth, T. E. Cowan, M. H. Key, S. P. Hatchett, C. Brown, W. Fountain, J. Johnson, D. M. Pennington, R. A. Snavely, S. C. Wilks, K. Yasuike, H. Ruhl, F. Pegoraro, S. V. Bulanov, E. M. Campbell, M. D. Perry, and H. Powell, *Phys. Rev. Lett.* **86**, 436 (2001).

[15]M. Roth, D. Jung, K. Falk, N. Guler, O. Deppert, M. Devlin, A. Favalli, J. Fernandez, D. Gautier, M. Geissel, R. Haight, C. E. Hamilton, B. M. Hegelich, R. P. Johnson, F. Merrill, G. Schaumann, K. Schoenberg, M. Schollmeier, T. Shimada, T. Taddeucci, J. L. Tybo, F. Wagner, S. A. Wender, C. H. Wilde, and G. A. Wurden, *Phys. Rev. Lett.* **110**, 044802 (2013).

[16]F. Nürnberg, I. Alber, K. Harres, M. Schollmeier, W. Barth, H. Eickhoff, I. Hofmann, A. Friedman, D.P. Grote, B.G. Logan, and M. Roth, *Journal of Physics: Conference Series* **244**, 022052 (2010).

[17] H. Chen, S. C. Wilks, J. D. Bonlie, S. N. Chen, K. V. Cone, L. N. Elberson, G. Gregori, D. D. Meyerhofer, J. Myatt, D. F. Price, M. B. Schneider, R. Shepherd, D. C. Stafford, R. Tommasini, R. Van Maren, and P. Beiersdorfer, *Phys. Plasmas,***16**, 122702 (2009).

[18]Ingo Hofmann, Ju¨rgenMeyer-ter-Vehn, XueqingY and HusamAl-Omarif, *Nuclear Instruments and Methods in Physics Research A*, **681** 44–54 (2012).

[19]A. Snavely, B. Zhang, K. Akli, Z. Chen, R. R. Freeman, P. Gu, S. P. Hatchett, D. Hey, J. Hill, M. H. Key, Y. Izawa, J. King, Y. Kitagawa, R. Kodama, A. B. Langdon, B. F. Lasinski, A. Lei, A. J. MacKinnon, P. Patel, R. Stephens, M. Tampo, K. A. Tanaka, R. Town, Y. Toyama, T. Tsutsumi, S. C. Wilks, T. Yabuuchi, and J. Zheng, *Phys. Plasmas* **14,** 092703 (2007).

[20]R. Sonobe, S. Kawata, S. Miyazaki, M. Nakamura, and T. Kikuchi, *Phys. Plasmas* **12**,

073104 (2005).

[21]S. Kawata, T. Izumiyama, T. Nagashima, M. Takanao, D. Barada, Q. Kong, Y. J. Gu, P. X. Wang, Y. Y. Ma and W. M. Wang, *Laser Therapy*], **22**, No. 2 (2013).

[22]Ute Linz and Jose Alonso, *Phys. Rev. ST Accel. Beams* **10**, 094801 (2007).

[23]Lund S.M, Cohen, R.H, Ni, P.A, *Phys. Rev. ST Accel. Beams* **16**, 044202 (2013).

[24]P.A. Ni, B.G. Logana1, S.M. Lund, N. Alexander, F.M. Bieniosek, R.H. Cohen, M. Roth and G. Schaumann, *Laser and Particle Beams*, **31,** pp 81-88 (2012).

[25]P. F. Ottinger, F. C. Young, S. J. Stephanakis, D. V. Rose, J. M. Neri, B. V. Weber1, M. C. Myers, D. D. Hinshelwood, D. Mosher, C. L. Olson, and D. R. Welch, *Phys. Plasmas*, **7**, 346 (2000).

[26]S. C. Wilks, A. B. Langdon, T. E. Cowan, M. Roth, M. Singh, *Phys. Plasma* **8**, 542 (2001).

[27] T. E. Cowan, J. Fuchs, H. Ruhl, A. Kemp, P. Audebert, M. Roth, R. Stephens, I. Barton, A. Blazevic, E. Brambrink, J. Cobble, J. Fernández, J.-C. Gauthier, M. Geissel, M. Hegelich, J. Kaae, S. Karsch, G. P. Le Sage, S. Letzring, M. Manclossi, S. Meyroneinc, A. Newkirk, H. Pépin, and N. Renard-LeGalloudec, *Phys. Rev. Lett.* **92**, 204801 (2004).

[28]C. Bellei, M. E. Foord, T. Bartal, M. H. Key, H. S. McLean, P. K. Patel, R. B. Stephens, and F. N. Beg, *Phys. Plasmas* **19**, 033109 (2012).

[29]F. Nürnberg, M. Schollmeier, E. Brambrink, A. Blazevic, D. C. Carroll, K. Flippo, D. C. Gautier, M. Geißel, K. Harres, B. M. Hegelich, O. Lundh, K. Markey, P. McKenna, D. Neely, J. Schreiber, and M. Roth, *Review of Scientific Instruments* **80** 033301 (2009).

[30]R.F. Hubbard, S.A. Goldstein, and D.A. Tidman, "Knock-on electrons in the target chamber," *Proceedings of the Heavy Ion Fusion Workshop*, Berkeley, California (1979).

[31]A. Frank, A. Blažević, V. Bagnoud, M. M. Basko, M. Börner, W. Cayzac, D. Kraus, T. Heßling, D. H. H. Hoffmann, A. Ortner, A. Otten, A. Pelka, D. Pepler, D. Schumacher, An. Tauschwitz, and M. Roth, Energy Loss and Charge Transfer of Argon in a Laser-Generated Carbon Plasma,Phys. Rev. Lett. **110**, 115001 (2013).

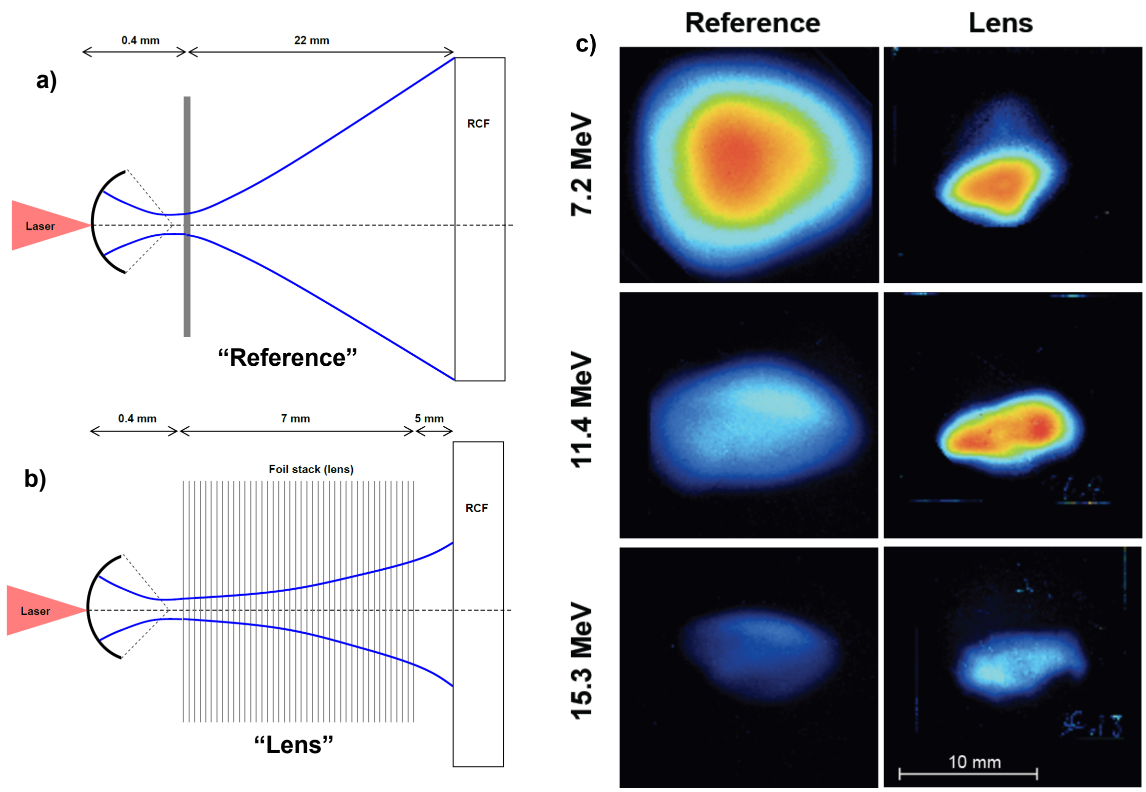

Figure 1: Setup of a reference experiment (a) and a lens experiment (b); dimensions are not to scale. Size of proton beam on RCF films at various energies (c). Images (optical density) are shown in false colors; spatial and intensity profiles are adjusted for a direct comparison. See more details in text.

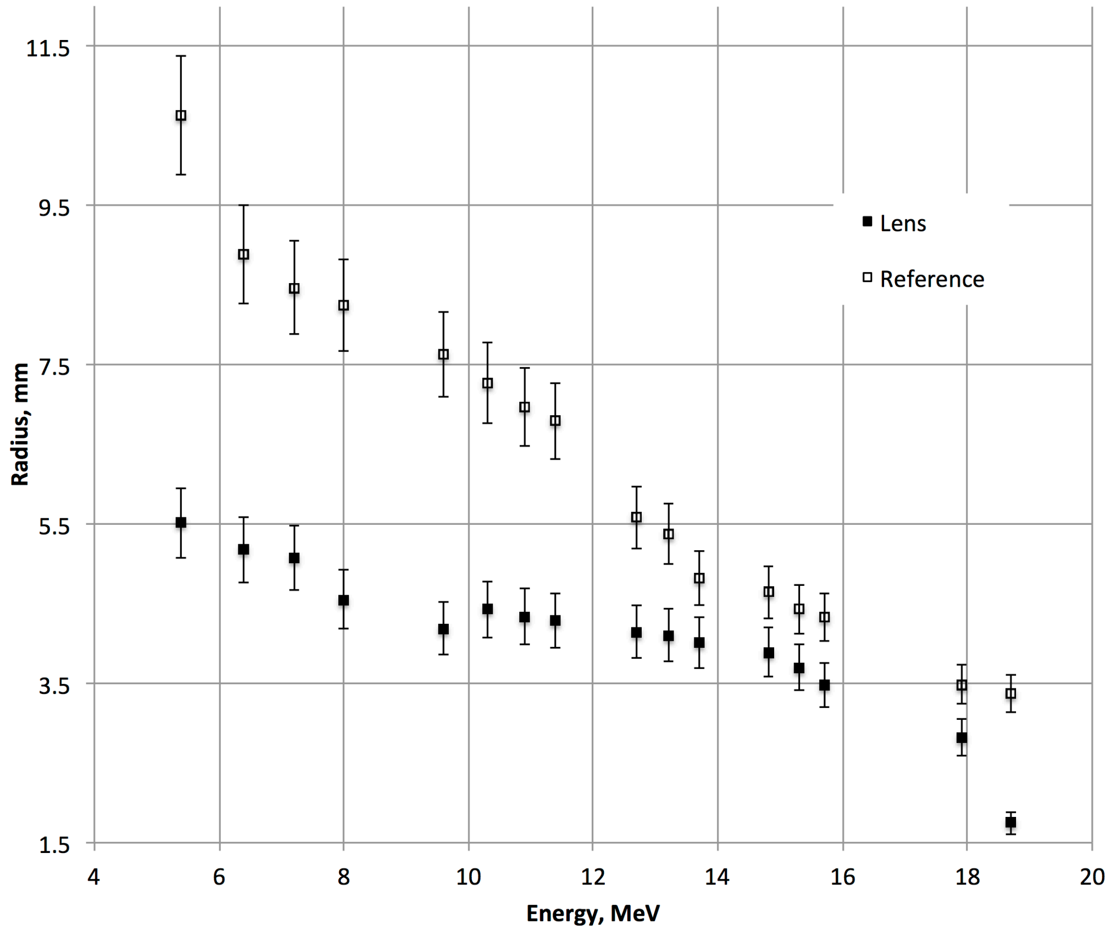

Figure 2: The average beam radius measured in single shots of the lens and reference targets.

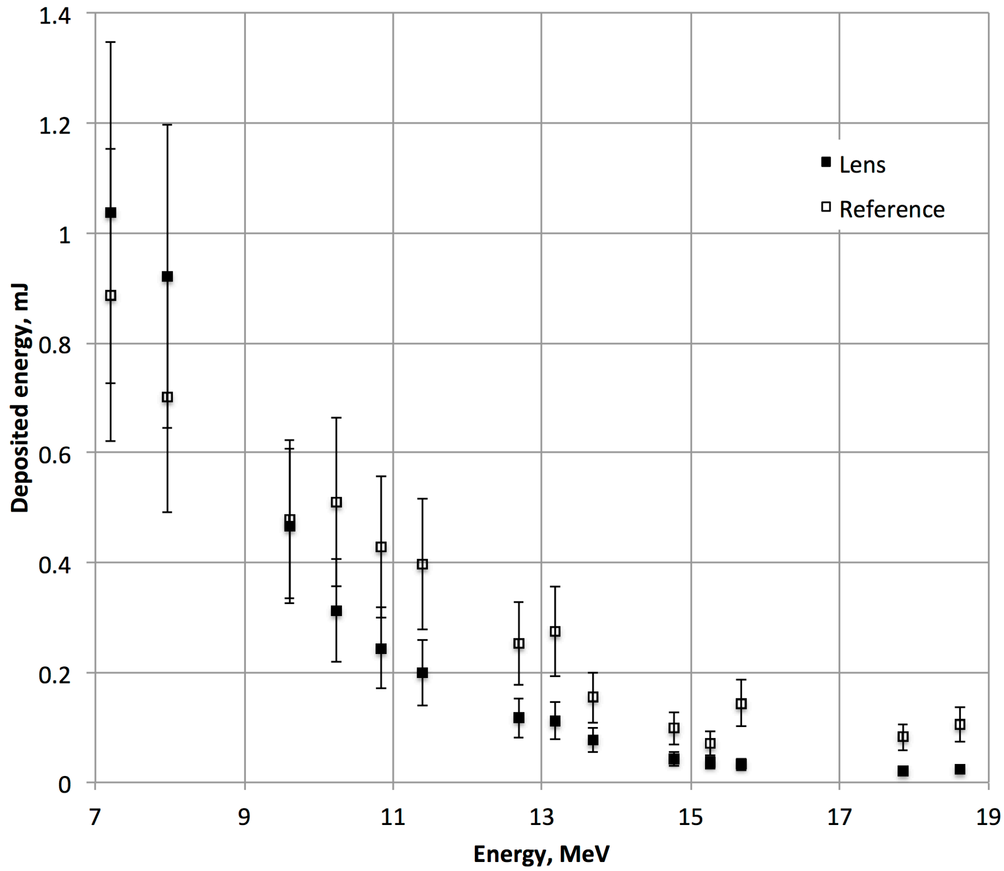

Figure 3: Energy deposited in the active layer (7 μm) of each RCF film in single shots of the lens and reference targets.

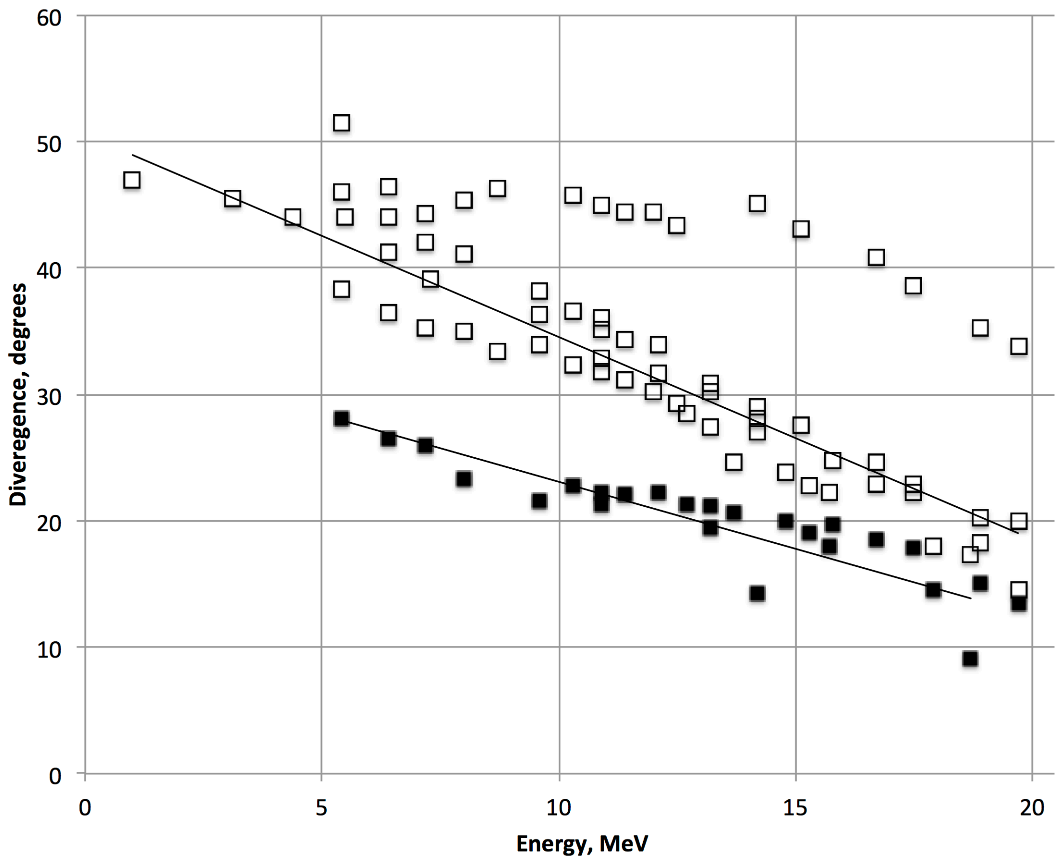

Figure 4: Effective divergence in multiple experiments demonstrates reproducibility of the phenomena. Solid squares -- lens shots; empty squares – reference shots.